0273-2289/96/6002—0123$09.00

Antigen-Antibody Binding Kinetics for Biosensors

Changes in the Fractal Dimension (Surface Roughness) and in the Binding Rate Coefficient

AJIT SADANA* AND ARUNA BEELA RAM

Chemical Engineering Department, University of Mississippi, University, MS 38677-9740

Received July 19, 1995; Accepted August 18, 1995

ABSTRACT

The diffusion-limited binding kinetics of antigen in solution to antibody immobilized on a biosensor surface is analyzed within a fractal framework. Changes in the fractal dimension, D_f observed are in the same and in the reverse directions as the forward binding rate coefficient k. For example, an increase in the concentration of the isoenzyme human creatine kinase isoenzyme MB form (CK-MB) (antigen) solution from 0.1 to 50 ng/mL and bound to anti-CK-MB antibody immobilized on fused silica fiber rods leads to increases in the fractal dimension D_f from 0.294 to 0.5080, and in the forward binding rate coefficient k from 0.1194 to 9.716, respectively. The error in the fractal dimension D_f decreases with an increase in the CK-MB isoenzyme concentration in solution. An increase in the concentration of human chorionic gonadotrophin (hCG) in solution from 4000 to 6000 mIU/mL hCG and bound to anti-hCG antibody immobilized on a fluorescence capillary fill device leads to a decrease in the fractal dimension D_f from 2.6806 to 2.6164, and to an increase in the forward binding rate coefficient k from 3.571 to 4.033, respectively. The different examples analyzed and presented together indicate one means by which the forward binding rate coefficient k may be controlled, that is by changing the fractal dimension or the 'disorder' on the surface. The analysis should assist in helping to improve the stability, the sensitivity, and the response time of biosensors.

*Author to whom all correspondence and reprint requests should be addressed.

Index Entries: Antigen-antibody binding kinetics; fractals.

INTRODUCTION

Sensitive detection systems are required to distinguish a wide range of substances. Sensors find application in the areas of biotechnology, physics, chemistry, medicine, aviation, oceanography, and environmental control. It is of tremendous interest to help characterize and to delineate the reactions occurring at the biosensor surface in order that one may enhance the sensitivity, specificity, stability, and reaction time of biosensors. The solid-phase immunoassay technique wherein the antigen in solution binds to an antibody-coated biosensor surface (or vice-versa), is a convenient method since the binding process is sensed directly and rapidly.

The kinetics of antigen-antibody binding play an important role in biosensor development, and as expected, considerable effort has been expended to analyze the classical role of diffusion and reaction at biosensor surfaces (*1–8*).

There are limitations to classical modelling techniques which do not account for heterogeneity at the reaction surface. Douglas (*9*) emphasizes that naturally occurring surfaces (cell membranes and organelles, soils, colloidal aggregates, and so on) tend to be highly irregular and need to be characterized appropriately. It is to be reasonably anticipated that the immobilization procedure utilized to attach the antigen or antibody to the biosensor surface would yield an irregular surface.

Mandelbrot (*10*) indicates that the fractal dimension provides a useful zeroth-order measure of the degree of surface roughness. These fractal functions provide reasonable qualitative and quantitative model surfaces for the analytic calculations of random walks interacting with rough surfaces. Kopelman (*11*) indicates that surface diffusion-controlled reactions that occur on clusters or islands are expected to exhibit anomalous and fractal-like kinetics. These fractal kinetics exhibit anomalous reaction orders and time-dependent rate (e.g., binding) coefficients. Fractals are disordered systems, and the disorder is described by nonintegral dimensions (*12*). These authors further indicate that as long as surface irregularities show scale invariance that is dilatational symmetry they can be characterized by a single number, the fractal dimension. The fractal dimension is a global property, and is insensitive to structural or morphological details (*13*).

Some studies have recently appeared that emphasize the spatio-temporal chaos that exists at reaction surfaces (*14,15*). Skinner (*14*) emphasizes that for chaos in biological systems only a few variables govern the spatial and temporal geometries of the system. An understanding of these fractional attractors or dimensions will significantly assist in the control of some of these complex systems. Furthermore, Friesen and

Laidlaw (*16*), while analyzing coal samples, indicate the possibility of the existence of two fractal dimensions that characterize a system or surface, and caution against well fitting the data (albeit incorrectly) by a single line or fractal dimension. Extreme care must be utilized to fit data, especially at the lower fractal dimensions.

Antibodies are heterogeneous and their immobilization on a fiber-optic surface, for example, would exhibit some degree of heterogeneity. This is a good example of a disordered system, and a fractal analysis is appropriate for such systems. Besides, the antibody-antigen reaction on the surface is a good example of a low-dimension reaction system in which the distribution tends to be less random (*11*). A fractal analysis would provide novel physical insights into the diffusion-controlled reactions occurring at the surface. Recently, Douglas et al. (*17*), while analyzing polymer adsorption and desorption to a surface, noted that the escape probability of a polymer is different if the surface is rough or fractal. Note that the desorption rate is related to the survival probability of a random walk initiating from the surface.

Fractal kinetics have been reported in other biochemical reactions, such as the gating of ion channels (*18,19*), enzyme reactions (*20*), and protein dynamics (*21*). The fractal nature has also been noted in the modeling of myosin heavy chain gene family (*22*), and in the self-similarity of 53 protein surfaces (*23*). The Buldyrev et al. (*22*) analysis is of interest since it suggests an increase in the fractal complexity of the myosin heavy chain gene with evolution with vertebrate > invertebrate > yeast. It has also been emphasized that the nonintegral dimensions of the Hill coefficient used to describe the allosteric effects of proteins and enzymes is a direct consequence of the fractal properties of proteins (*20*).

The fractal dimension values for the kinetics of the binding of antigen in solution to antibody immobilized on the biosensor surface are presented by reanalyzing data from experiments. More precisely, one would like to delineate the role of surface roughness on the speed of response, specificity, and sensitivity of fiber-optic immunosensors. Since the forward binding rate coefficient directly affects the above-mentioned parameters, it would be useful to relate the surface roughness to the forward binding rate coefficient.

THEORY

An analysis of the binding kinetics of antigen in solution to antibody immobilized on the biosensor surface is available (*5,6*). The influence of lateral interactions on the surface and variable rate coefficients is also available (*7*). Here we present a method of estimating actual fractal dimension values for antibody-antigen binding systems utilized in fiber-optic biosensors.

Variable Binding Rate Coefficient

Kopelman (*11*) has recently indicated that classical reaction kinetics is sometimes unsatisfactory when the reactants are spatially constrained on the microscopic level by either walls, phase boundaries, or force fields. Such heterogeneous reactions, for example, bioenzymatic reactions, that occur at interfaces of different phases exhibit fractal orders for elementary reactions and rate coefficients with temporal memories. In such reactions, the rate coefficient exhibits a form given by:

$$k_1 = k' t^{-b} \qquad O < b < 1 (t = 1) \tag{1a}$$

In general, k_1 depends on time, whereas $k' = k_1 (t = 1)$ does not. Kopelman (*11*) indicates that in three dimensions (homogeneous space), b equals zero. This is in agreement with the results obtained in classical kinetics. Also, with vigorous stirring, the system is made homogeneous and b again equals zero. However, for diffusion-limited reactions occurring in fractal spaces, $b > 0$; this yields a time-dependent rate coefficient.

The random fluctuations on a two-state process in ligand binding kinetics has been analyzed (*24*). The stochastic approach can be used as a means to explain the variable binding rate coefficient. The simplest way to model these fluctuations is to assume that the binding rate coefficient $k_1 (t)$ is the sum of its deterministic value (invariant) and the fluctuation $[z (t)]$ (*24*). This $z (t)$ is a random function with a zero mean. The decreasing and increasing binding rate coefficients can be assumed to exhibit an exponential form (*5–7, 25*):

$$\begin{aligned} k_1 &= k_{1,0} \exp (-\beta t) \\ k_1 &= k_{1,0} \exp (\beta t) \end{aligned} \tag{1b}$$

Here, β and $k_{1,0}$ are constants.

Sadana and Madagula (*7*) have analyzed the influence of a decreasing and an increasing binding rate coefficient on the antigen concentration near the surface when the antibody is immobilized on the surface. The authors noted that for an increasing binding rate coefficient, after a brief time interval as time increases, the concentration of the antigen near the surface decreases, as expected for the cases when lateral interactions are present or absent. The diffusion-limited binding kinetics of antigen (or antibody or substrate) in solution to antibody (or antigen or enzyme) immobilized on a biosensor surface has been analyzed within a fractal framework (*26,27*). Furthermore, experimental data presented for the binding of HIV virus (antigen) to the antibody anti-HIV immobilized on a surface displays a characteristic ordered "disorder" (*28*). This indicates the possibility of a fractal-like surface. It is obvious that the above biosen-

sor system (wherein either the antigen or the antibody is attached to the surface) along with its different complexities that include heterogeneities on the surface and in solution, diffusion-coupled reaction, time-varying adsorption, or binding rate coefficients, and so on, can be characterized as a fractal system.

The diffusion of reactants towards fractal surfaces has been analyzed (*29–31,13*). Havlin (*32*) has briefly reviewed and discussed the results. Sadana and Madagula (*7*) have recently presented a theoretical analysis using fractals for the time-dependent binding of antigen in solution to antibody immobilized on a fiber-optic biosensor surface. The authors noted that an increase in the fractal dimension utilized in their studies decreased both the rate of antigen binding and the amount of antigen bound.

Havlin (*32*) indicates that the diffusion of a particle (antibody [Ab]) from a homogeneous solution to a solid surface (antigen [Ag]-coated biosensor surface) where it reacts to form a product (antibody-antigen complex; Ab.Ag) is given by:

$$(\text{Ab.Ag}) \sim \begin{cases} t^{(3-D_f)/2} = t^p & t < t_c \\ t^{1/2} & t > t_c \end{cases} \qquad (2)$$

Here, D_f is the fractal dimension of the surface. Equation (2) indicates that the concentration of the product Ab.Ag (t) in a reaction Ab + Ag → Ab.Ag on a solid fractal surface scales at short and intermediate scales as Ab.Ag(t) ~ t^p with the coefficient $p = (3\text{-}D_f)/2$ at short time scales, and $p = 1/2$ at intermediate time scales. This equation is associated to the short term diffusional properties of a random walk on a fractal surface. Note that in a perfectly stirred kinetics on a regular (nonfractal) structure (or surface), k_1 is a constant, that is, it is independent of time. In other words, the limit of regular structures (or surfaces) and the absence of diffusion-limited kinetics leads to k_1 being independent of time. In all other situations one would expect a scaling behavior given by $k_1 \sim k' t^{-b}$ with $-b = p < 0$. Also, the apprearance of the coefficient, p different from $p = 0$ is the consequence of two different phenomena, that is the heterogeneity (fractality) of the surface, and the imperfect mixing (diffusion-limited condition). Havlin (*32*) indicates that the crossover value may be determined by $r_c^2 \sim t_c$. Above the characteristic length, r_c, the self-similarity of the surface is lost. Above t_c, the surface may be considered homogeneous, since the self-similarity property disappears and regular diffusion is now present. For the present analysis, t_c is arbitrarily chosen. One may consider the analysis to be presented as an intermediate "heurisitic" approach in that in the future one may also be able to develop an autonomous (and not time-dependent) model of diffusion-controlled kinetics in disordered media.

RESULTS

Increase in the Fractal Dimension and in the Forward Binding Rate Coefficient

Walczak et al. (33) have recently developed an evanescent fiber-optic biosensor to analyze the human enzyme creatine kinase (CK: EC 2.7.3.2) isoenzyme MB form (CK-MB) with a molecular weight of about 84,000. Custom β-phycoerythrin CK-MB antibody conjugates were immobilized on fused silica fiber-optic sensors. There is considerable interest in the development of a biosensor for the detection of the above cardiac isoenzyme since it permits an early detection of myocardial infarctions. Figure 1A–D shows the curves obtained using Eq. (2) for the binding of the CK-MB isoenzyme. Table 1 shows the values of the parameters k, p, and D_f obtained using Eq. (2), a biphasic function of time, to model the experimental data. The parameter values presented in Table 1 were obtained from a regression analysis using Sigmaplot (34) to model the experimental data using Eq. (2), wherein (Ab.Ag) = kt^p. The k, p, and D_f values presented in Table 1 are within 95% confidence limits. This indicates that the determined values are reliable and significant. The Sigmaplot program provided the ± values for k and p. The errors or shifts in D_f were obtained from the ± values of p. The values of the shifts in D_f are twice that of p, since $[(3 - D_f)/2]$ equals p. Table 1 shows that the fractal dimension, D_f increases from 0.2004 (the lowest value in the range utilized) to 0.5240 as the initial concentration of the isoenzyme in solution increases from 0.1 to 50 ng/mL. The fractal dimension increases by about a factor of 16 as the initial concentration of the isoenzyme in solution increases by a factor of 500. For this same change in CK-MB isoenzyme concentration in solution, the forward binding rate coefficient k changes by a factor of about 81 from 0.1194 to 9.716. Note that the change in the forward binding rate coefficient k is in the same direction as that of the fractal dimension D_f.

The curves in Figs. 1A–D, 2A–b, and 3 are theoretical curves. More refined fits could have been obtained if a multifractal analysis instead of a single-fractal analysis was used to model the data in Fig. 1A and B and for other data analysis to be presented in later figures. Multifractal dimensions have been indicated in adsorption (35), and for other systems (15). Such an analysis was not presented here since for the present, based on the current state of knowledge, we feel that a single fractal dimension analysis is sufficient to adequately describe the antigen-antibody binding kinetics for the binding systems analyzed. For example, in Fig. 1A the theoretical curve continues upward whereas the data shows the values in fluorescence leveling off after time. In this case a dual fractal dimension would fit the data better. Also, the value of the first fractal dimension (that is, closer to time, $t = 0$) would be smaller than that of the second fractal dimension. The second fractal dimension starts about when the

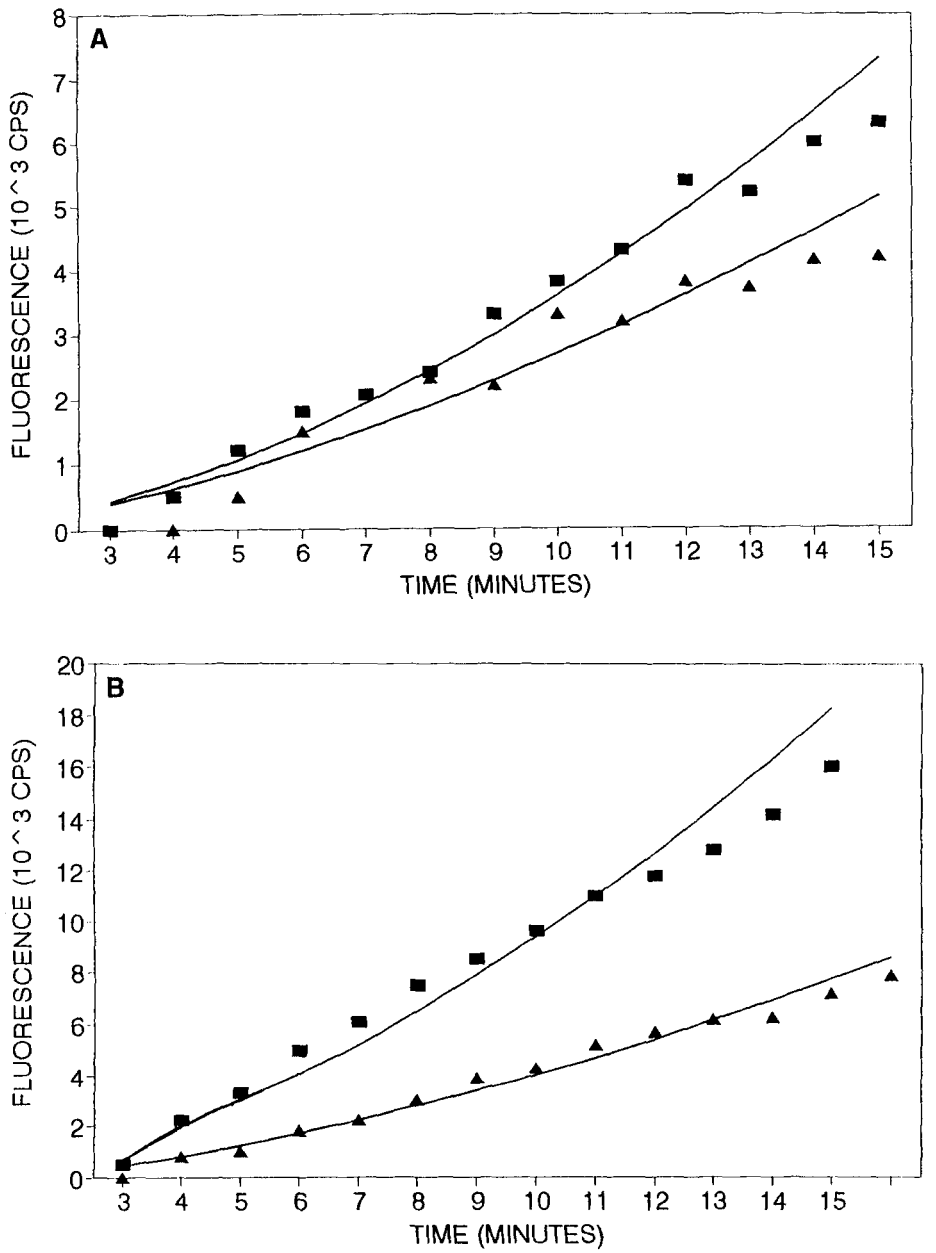

Fig. 1. Influence of isoenzyme concentration in solution on the binding rate curves for human creatine kinase isoenzyme (CK-MB) to antibody immobilized on a fiber-optic biosensor surface (33). Isoenzyme concentration: (**A**) ▲ 0.1 ng/mL; ■ 0.5 ng/mL; (**B**) ▲ 1.0 ng/mL; ■ 2.0 ng/mL.

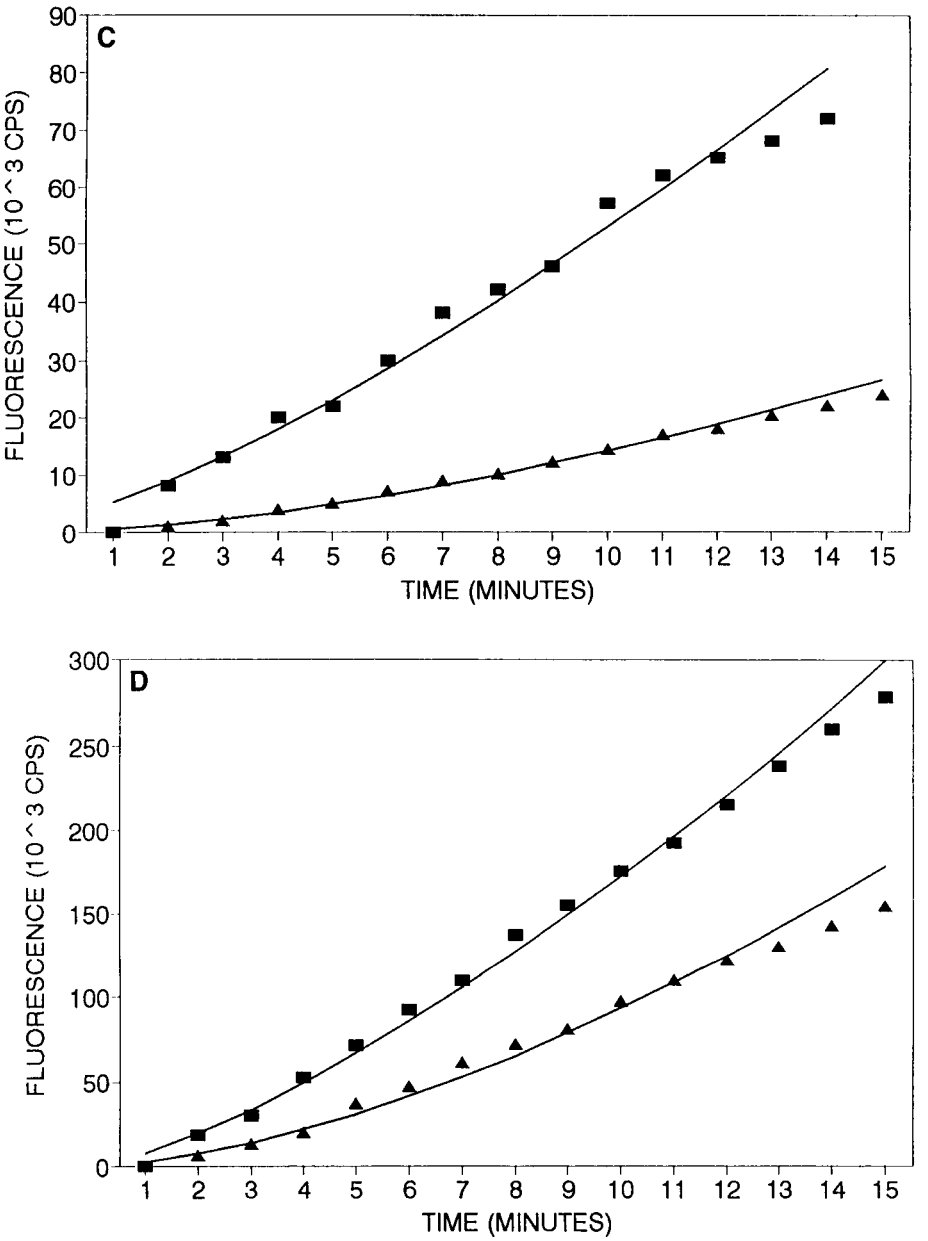

Fig. 1. (*cont'd*). (C) ▲ 5.0 ng/mL; ■ 10 ng/mL; (D) ▲ 20 ng/mL; ■ 50 ng/mL.

values in fluorescence start to level off. This is also physically consistent in that the state of disorder has increased with time. A similar explanation applies to Fig. 1B where the top curve shows an S-shape curve. Here too a dual-fractal dimension would provide a better fit. Once again the value of the second fractal dimension would be higher than that of the first fractal dimension.

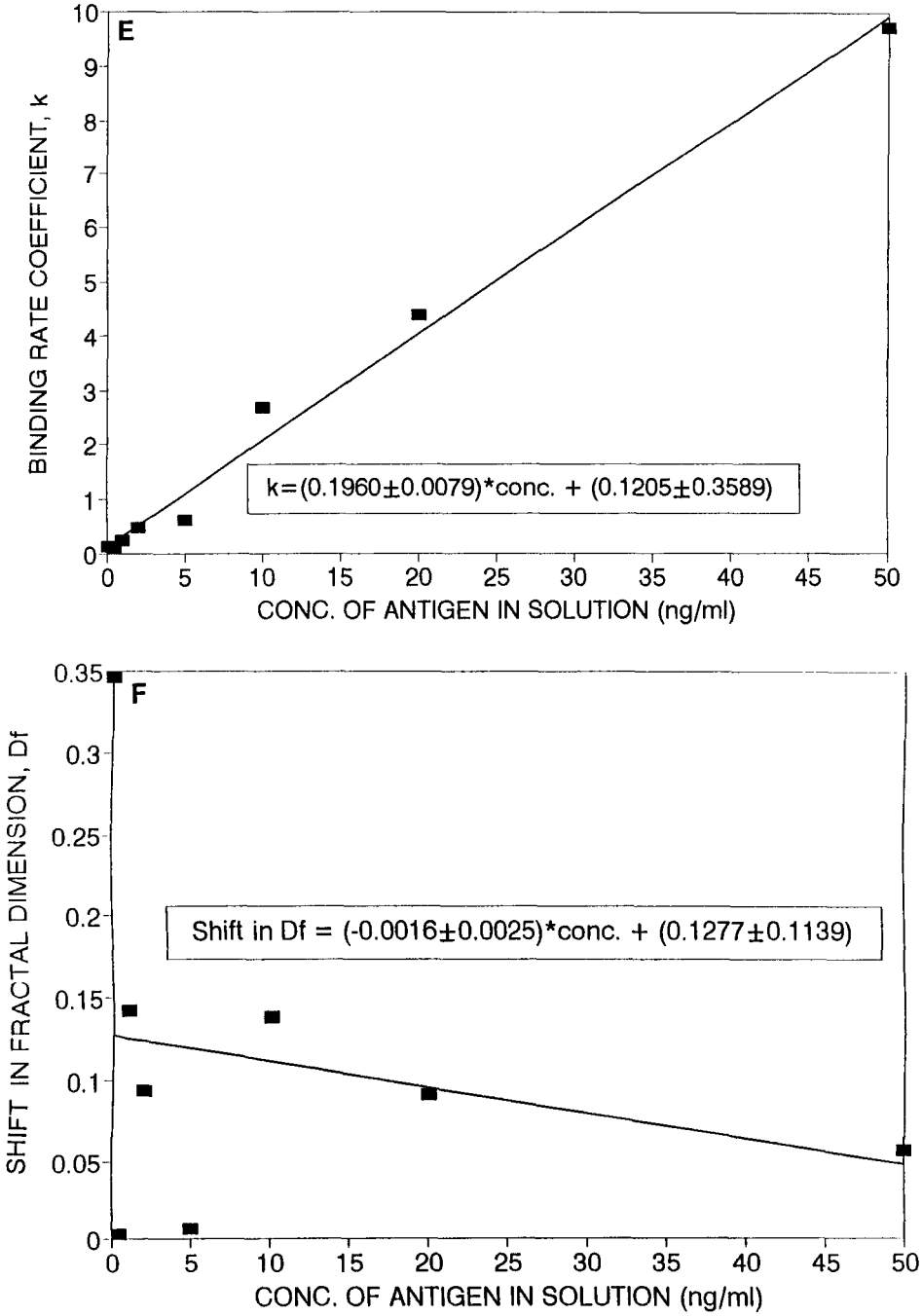

Fig. 1. (*cont'd*). (**E**) Linear increase in the forward binding rate coefficient k with an increase in the CK-MB isoenzyme concentration in solution; (**F**) Decrease in the error (shift) of the fractal dimension D_f with an increase in the CK-MB isoenzyme concentration in solution.

Table 1
Fractal Dimension Df and Binding Rate Coefficient k Values for Different Antigen-Antibody Binding Systems

Antigen in solution	Antibody on surface	Type of immunosensor	Immobilization procedure	k	p	Df	Ref.
(a) Human creatine kinase (CK; EC 2.7.3.2) isoenzyme MB form; 50ng/mL)	Anti-CK-MB	Fluorometric evanescent immunosensor	100 g/mL antibody solution adsorbed on silanized 1.00 mm diameter fused silica fiber rods	9.716 ± 0.6741	1.246 ± 0.0281	0.5080 ± 0.0562	(33)
CK-MB; 20 ng/mL	Anti-CK-MB	same as above	same as above	4.388 ± 0.4977	1.326 ± 0.0497	0.3480 ± 0.0915	(33)
CK-MB; 10 ng/mL	Anti-CK-MB	same as above	same as above	2.679 ± 0.4574	1.238 ± 0.069	0.5240 ± 0.1388	(33)
CK-MB; 5 ng/mL	Anti-CK-MB	same as above	same as above	0.620 ± 0.0514	1.359 ± 0.033	0.2820 ± 0.0067	(33)
CK-MB; 2 ng/mL	Anti-CK-MB	same as above	same as above	0.466 ± 0.0544	1.303 ± 0.047	0.3940 ± 0.094	(33)
CK-MB; 1 ng/mL	Anti-CK-MB	same as above	same as above	0.233 ± 0.0413	1.308 ± 0.0713	0.3010 ± 0.1427	(33)
CK-MB; 0.5 ng/mL	Anti-CK-MB	same as above	same as above	0.1102 ± 0.0277	1.516 ± 0.100	0.2002 ± 0.003	(33)
CK-MB; 0.1 ng/mL	Anti-CK-MB	same as above	same as above	0.1194 ± 0.0517	1.353 ± 0.1729	0.294 ± 0.3458	(33)
(b) Progesterone: sensor 1	P-Ab	Competitive enzyme immunoassay	Sodium periodate method	1.369 ± 0.1605	0.1813 ± 0.0293	2.637 ± 0.1170	(36)
Progesterone; sensor 2	P-Ab	same as above	same as above	0.8254 ± 0.077	0.2149 ± 0.0231	2.570 ± 0.0462	(36)
Progesterone; sensor 2	P-Ab	same as above	same as above	0.0434 ± 0.018	0.7128 ± 0.0892	1.425 ± 0.1783	(36)
(c) Human chorionic gonadotrophin (hCG) in serum; 502 mIU/mL hCG	anti-hCG	fluorescence capillary fill device (FCFD)	antibody on lower plate of device	2.758 ± 0.178	0.1171 ± 0.0269	2.766 ± 0.054	(37)
hCG in serum; 4000 mIU/mL hCG	anti-hCG	FCFD	same as above	3.571 ± 0.191	0.1597 ± 0.0222	2.681 ± 0.0444	(37)
hCG in whole blood; 6000 mIU/mL hCG	anti-hCG	FCFD	same as above	4.033 ± 0.436	0.1918 ± 0.0426	2.616 ± 0.0852	(37)

Figure 1E shows that the forward binding rate coefficient k increases linearly as the CK-MB isoenzyme concentration in solution increases from 0.1 to 50 ng/mL. Fractal dimension values close to one indicate that the antibodies are arranged in lines on the surface. Fractal dimension values increasingly greater than one indicate a higher "ruggedness" for the system. Fractal dimension values less than one are rather rare. It may be suggested that for fractal dimension values less than one the antibodies are arranged in lines or even sparser patterns on the biosensor surface. Partially blocked active sites on the antibodies arranged in lines could also yield fractal dimension values less than one (*13*). The low values of the fractal dimension obtained for this CK-MB isoenzyme (0.2004 to 0.5240) suggests a Cantor-like dust as the antibody-CK-MB isoenzyme interface.

Table 1 indicates that the shift in the fractal dimension increases as the concentration of the CK-MB enzyme in solution decreases. Figure 1F shows clearly that the shift in the fractal dimension D_f decreases as the CK-MB isoenzyme concentration in solution increases. One could fit almost any curve to the data. However, there is a significant increase in the shift in the fractal dimension at the lower CK-MB isoenzyme concentrations. This indicates a significant amount of inhomogeneity in the state of disorder of the antibody-isoenzyme binding system at the lower CK-MB isoenzyme concentrations. The higher relative shifts in the fractal dimension D_f exhibited at the lower CK-MB concentrations may indicate the existence of a dual- or multifractal surface. This type of surface may be described by more than just a single attractor (*15*). Spatio-temporal chaos is known to exist for other systems wherein a large number of chaotic elements distributed in space are required to describe the system (*15*). Also, at the lower CK-MB isoenzyme concentrations, nonspecific binding of the CK-MB isoenzyme to the fiber-optic biosensor surface could play an important role relative to specific binding of the CK-MB isoenzyme to the antibody, anti-CK-MB. This is one possible explanation for the significant shifts in the fractal dimension, D_f observed at the lower CK-MB isoenzyme concentrations.

Schramm and Paek (*36*) have developed a heterogeneous competitive immunoassay for the continuous monitoring of steroid hormone progesterone. They immobilized two antibodies on spatially different areas. Antibody 1 and 2 are bound to sensor 1 and 2, respectively. Antibody 1 binds to the analyte and antibody 2 binds to an enzyme (horseradish peroxidase). The analyte-enzyme complex serves as a heterobifunctional shuttle and is the signal generator. Figure 2A shows the curves obtained using Eq. (2) for the binding of progesterone to sensor 1. Table 1B indicates that the forward binding rate coefficient k is 1.369, and the fractal dimension D_f value is 2.637. This is a high value of the fractal dimension D_f and indicates a significant amount of inhomogeneity or state of disorder on the biosensor surface.

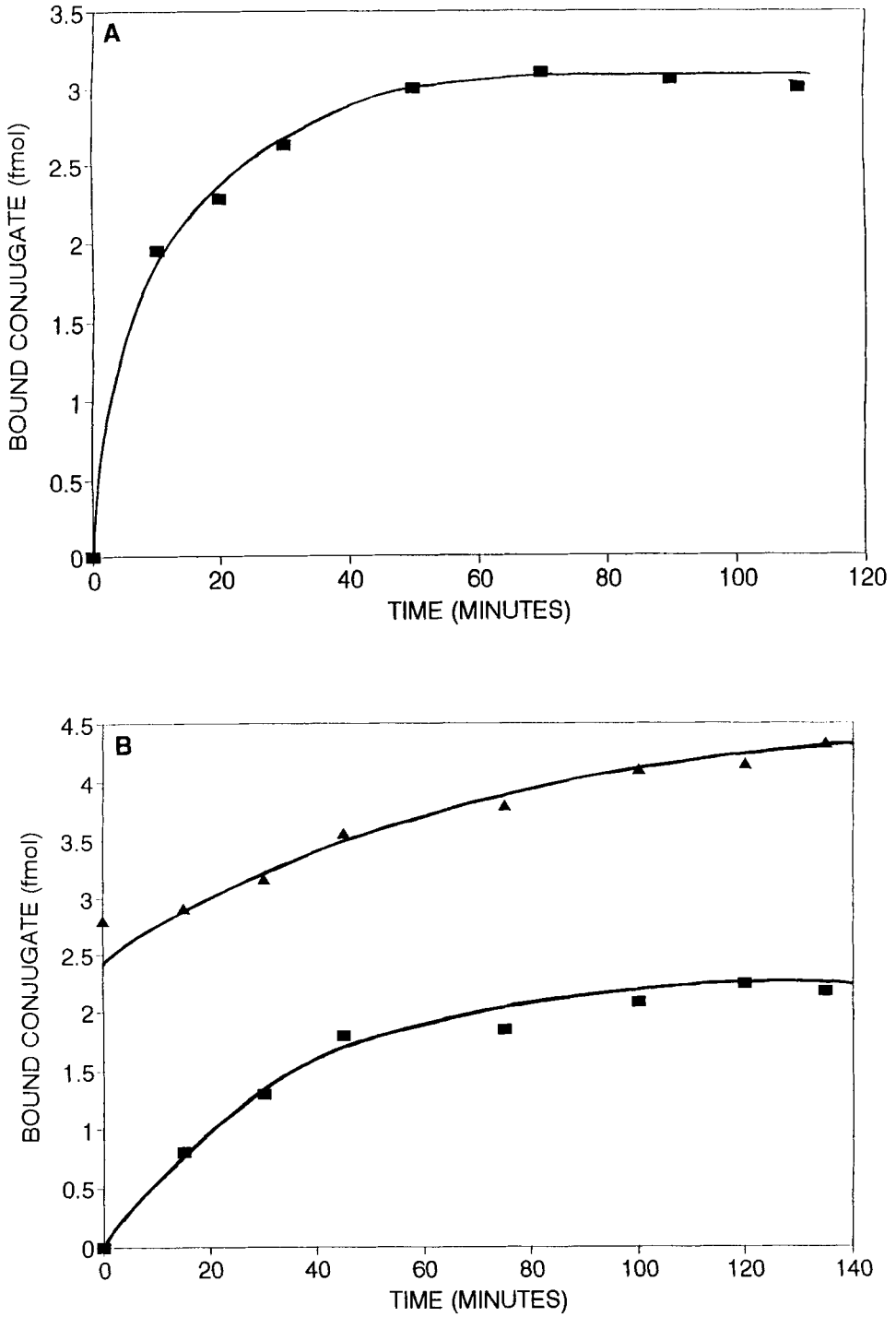

Fig. 2. Binding rate curves for progesterone to: (**A**) Sensor 1; (**B**) Sensor 2: ■ establishment of equilibrium conditions; ▲ changes in the analyte concentration.

Figure 2B shows the curves obtained using Eq. (2) for the binding of progesterone to sensor 2 for two cases. One is during the establishment of equilibrium, and the other is for the response of the heterobifunctional analyte to changes (increases) in the analyte concentration. Table 1B shows the values of the binding rate coefficient k, and of the fractal dimension D_f, for the two cases analyzed. Note that for sensor 2 as the fractal dimension D_f decreases from 2.670 to 1.426 (representing a change of 46.5%) the forward binding rate coefficient k decreases by a factor of 19 from a value of 0.8254 to 0.0434. In this case the forward binding rate coefficient k is rather sensitive to the fractal dimension D_f. One should note that we are talking of two separate stages during the process of sensing. Also, the fractal dimension D_f value of 2.570 obtained during the equilibrium process does indicate a high level of inhomogeneity or state of disorder on the sensor 2 surface. It is of interest to note that for sensor 2 the changes in the forward binding rate coefficient k and in the fractal dimension D_f, are in the same direction. Note that the values of the binding rate coefficient k are 1.369 and 0.8254 for sensors 1 and 2, respectively. Also, the fractal dimension D_f values are 2.637 and 2.570 for sensors 1 and 2, respectively. In this case, even when we go from sensor 1 to 2 the changes in the fractal dimension D_f and in the forward binding rate coefficient k are in the same direction.

Decrease in the Fractal Dimension D_f, and Increase in the Binding Rate Coefficient k

Deacon et al. (37) have recently developed a fluorescence capillary fill device (FCFD) as an immunosensor for the detection of hCG. These authors indicate that detectable amounts of hCG appear shortly after conception. hCG levels reach a peak at about three months of gestation. Also, hCG may be present due to certain kinds of tumors (for example, testicular carcinoma) in the human body. Anti-hCG antibodies were utilized for the hCG sandwich immunoassay in the FCFD deviceds. Figure 3A and B shows the curves obtained using Eq. (2) for the binding of hCG in serum and in blood samples. Table 1 shows that the fractal dimension D_f decreases (by about 3.1%) from 2.7660 to 2.6806 as the hCG concentration in the serum sample increases by about a factor of 8 from 502 to 4000 mIU/mL hCG. This represents only a slight decrease in the state of disorder as the hCG concentration increases by a factor of about 8. The fractal dimension D_f values obtained are relatively high. This represents a high state of disorder or ruggedness or inhomogeneity for both of the hCG concentrations utilized. Note that the forward binding rate coefficient k value increases by 29.4% from 2.758 to 3.571 as the hCG concentration in solution increases by a factor of about 8 from 520 to 4000 mIU/mL hCG. In this case note that the changes in the fractal dimension D_f and in the forward binding rate coefficient k are in the reverse direction.

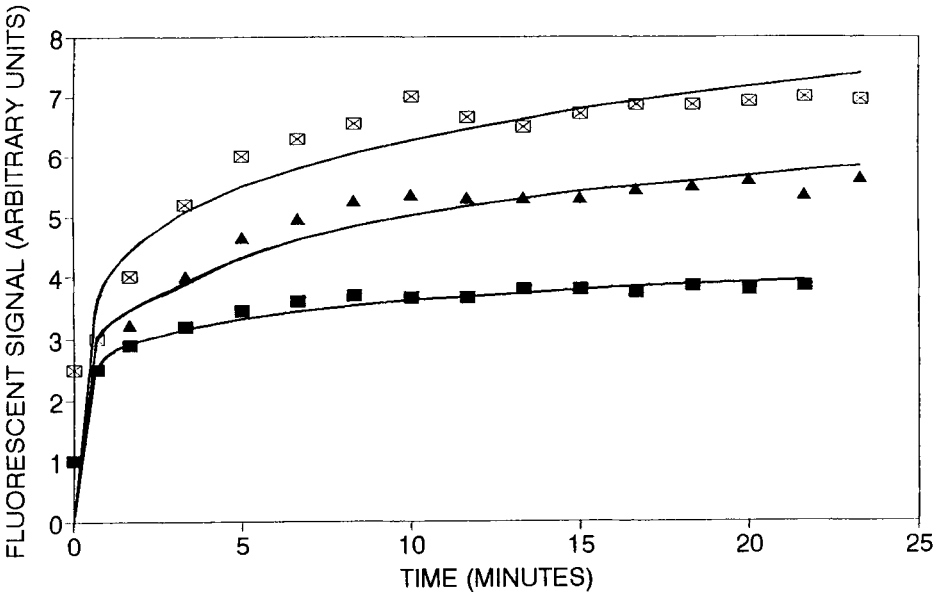

Fig. 3. Binding rate curves for human chorionic gonadotrophin (hCG) in serum and in blood samples to antibody immobilized to a surface in a fluorescence capillary fill device (FCFD) (37): serum sample: ■ 502 mIU/mL hCG; ▲ 4000 mIU/mL hCG; blood sample: ☒ 6000 mIU/mL hCG.

Table 1 also shows the D_f value of 2.6164 obtained for the single concentration of 6000 mIU/mL hCG in blood solution presented. The forward binding rate coefficient k value obtained is 4.033. It is not very appropriate to do so since we are comparing two different types of solutions. Nevertheless, one notes that the forward binding rate coefficient k increases by about 11.4% from a value of 3.571 to 4.033, and the fractal dimension D_f decreases by about 2.2% from a value of 2.6806 to 2.6264 as one goes from 4000 mIU/mL hCG in serum to 6000 mIU/mL hCG in blood samples. Once again, the changes in the fractal dimension D_f and in the forward binding rate coefficient k are in the reverse direction. This result should, of course, be viewed with caution since we are comparing the binding of hCG from two different types of solutions.

CONCLUSIONS

The fractal analysis of the binding of the antigen in solution to the antibody immobilized on the biosensor surface provides a quantitative indication of the state of disorder on the surface. Changes in the fractal dimension D_f observed are in the same and in the reverse directions as the forward binding rate coefficient k. In other words, in some cases the state of disorder on the surface is beneficial for the forward binding rate coefficient k, and in some cases it is not. There is direct (27) and indirect

evidence (*17*) to suggest that an increasing roughness on the surface would tend to increase the adsorption or binding rate coefficient. Further analysis is required to delineate the decrease in the forward binding rate coefficient k with an increase in the fractal dimension D_f. This is especially so for those cases where there is no change in the biosensor system except for a variable change such as the antigen or antibody concentration in solution. This behavior was observed for human chorionic gonadotrophin in solution. It is to be noted, however, that the change in the fractal dimension was rather low (3.1%).

Nonspecific binding plays a significant role in the antigen-antibody binding systems for biosensor applications. Our initial analysis indicates an increase in the shift in the fractal dimension D_f with a decrease in the creatine kinase isoenzyme concentration in solution. This increase in the shift in D_f is presumably due to a relatively increasing role played by nonspecific binding at the lower isoenzyme concentrations. Since the measurement of dilute concentrations of this isoenzyme and of other analytes is of interest, it would be helpful to be able to reduce the shift in the fractal dimension or the degree of spatio-temporal chaos that exists in these types of systems. A better control of the fractal dimension on the surface would significantly enhance the understanding of the sensitivity, stability, selectivity, and response time of biosensors.

REFERENCES

1. Bluestein, B. I., Craig, M., Slovacek, R., Stundtner, L., Uricouli, C., Walczak, I., and Luderer, A. (1991), in *Biosensors with Fiberoptics*, Wise, D., and Wingard, Jr., L. B., eds., Humana, Clifton, NJ, pp. 181–223.
2. Eddowes, M. J. (1987/1988), *Biosensors* **3,** 1–15.
3. Giaver, I. (1976), *J. Immunol.* **116,** 766–771.
4. Nygren, H. and Stenberg, M. (1985), *J. Colloid Interf. Sci. 1985* **107,** 560–566.
5. Sadana, A. and Sii, D. (1992a), *J. Colloid Interf. Sci.* **151 (1),** 166–177.
6. Sadana, A. and Sii, D. (1992b), *Biosensors Bioelectron* **7,** 559–568.
7. Sadana, A. and Madagula, A. (1993), *Biotechnol. Progr.* **9,** 259–266.
8. Stenberg, M. and Nygren, H. A. (1982), *Anal. Biochem.* **127,** 183–192.
9. Douglas, J. F. (1989), *Macromolecules* **22,** 3707–3716.
10. Mandelbrot, B. B. (1982), *The Fractal Geometry of Nature.* Freeman, San Francisco.
11. Kopelman, R. (1988), *Science* **241,** 1620–1626.
12. Pfeifer, P. and Obert, M. (1989), in *The Fractal Approach to Heterogeneous Chemistry: Surfaces, Colloids, Polymers,* Avnir, D., ed., Wiley, New York, pp. 11–43.
13. Nyikos, L. and Pajkossy, T. (1986), *Electrochim. Acta.* **31,** 1347–1350.
14. Skinner, J. E. (1994), *Bio/Technology 1994* **12,** 596–600.
15. Cross, M. C. and Hohenberg, P. C. (1994), *Science* **263,** 1569–1570.
16. Friesen, W. I. and Laidlaw, W. G. (1993), *J. Colloid Interf. Sci.* **160,** 226–235.
17. Douglas, J. F., Johnson, H. E., and Garnick, S. (1993), *Science* **242,** 2010–2012.
18. Liebovitch, L. S. and Sullivan, J. M. (1987a) *Biophys. J.* **52,** 979–988.
19. Liebovitch, L. S., Fischbarg, J., Koniarek, J. P., Todorova, I., and Wang, M. (1987b), *Math. Biosci.* **84,** 37–68.
20. Li, H., Chen, S., and Zhao, H. (1990), *Biophys. J.* **58,** 1313–1320.

21. Dewey, T. G. and Bann, J. G. (1992), *Biophys. J.* **63,** 594–598.
22. Buldyrev, S. V., Goldberger, A. L., Havlin, S., Peng, C. K., Stanley, H. E., Stanley, M. H. R., and Simons, M. (1993), *Biophys. J.* **65**, 2673–2679.
23. Goetze, T. and Brickmann, J. (1992), *Biophys. J.* **61,** 109–118.
24. Di Cera, E. (1991), *J. Chem. Phys.* **95 (7),** 5082–5086.
25. Cuypers, P. A., Willems, G. M., Kop, J. M., Corsel, J. W., Jansen, M. P., and Hermens, W. T. (1987), in *Proteins at Interfaces. Physicochemical and Biochemical Studies,* Brash, J. L., Horbett, Jr., T. A., eds., American Chemical Society, Washington, DC, pp. 208–211.
26. Sadana, A. and Beela Ram, A. (1994), *Biotechnol. Progr.* **10,** 291–298.
27. Sadana, A. (1995), *Biotechnol. Prog.* **11,** 50–57.
28. Anderson, J. NIH Panel Review Meeting, Case Western Reserve University, Cleveland, OH, July 1993.
29. De Gennes, P. G. (1982), *Radiat. Phys. Chem.* **22,** 193–196.
30. Pfeifer, P., Avnir, D., and Farin, D. J. (1984a), *Nature (London)* **308 (5956),** 261–263.
31. Pfeifer, P., Avnir, D., and Farin, D. J. (1984b), *J. Colloid Interf. Sci.* **103 (1),** 112–123.
32. Havlin, S. (1989), in *The Fractal Approach to Heterogeneous Chemistry: Surfaces, Colloids, Polymers,* Avnir, D., ed., Wiley, New York, NY, pp. 251–269.
33. Walczak, I. M., Love, W. F., Cook, T. A., and Slovacek, R. E. *Biosens. Bioelectron. 1992,* **7,** 39–48.
34. Sigmaplot (1993) Scientific Graphing Software, User's Manual, Jandel Scientific, San Rafael, CA.
35. Vlad, M. O. (1993), *J. Colloid Interf. Sci.* **159,** 21–27.
36. Schramm, W. and Paek, S. H. (1992), *Biosensors Bioelectron* **7,** 103–114.
37. Deacon, J. K., Thomson, A. M., Page, A. L., Stops, J. E., Roberts, P. R., Whiteley, S. C., Attridge, J. W., Love, C. A., Robinson, G. A., and Davidson, G. P. (1991), *Biosensors Bioelectron* **6,** 193–199.